applied sciences

MDPI

Article

Solidification of Radioactive Wastes Using Recycled Cement Originating from Decommissioned Nuclear-Energy Facilities

Ji-Hun Jeon [1], Jong-Hwan Lee [1], Woo-Chun Lee [1,2], Sang-Woo Lee [1,2] and Soon-Oh Kim [1,*]

[1] Department of Geology and Research Institute of Natural Science (RINS), Gyeongsang National University (GNU), Jinju 52828, Republic of Korea; jeonjh@gnu.ac.kr (J.-H.J.)
[2] HS Environmental Technology Research Center, Hosung Inc., Jinju 52818, Republic of Korea
* Correspondence: sokim@gnu.ac.kr

Abstract: Hundreds of thousands of tons of waste are generated from decommissioned nuclear-power facilities, and it has become a critical global issue to secure technology for reducing and recycling this waste. Concrete waste (CW) is estimated to comprise 60–80% of the total waste, and concrete-waste powder (CWP) includes enough inorganic substances used as effective materials for waste treatment. Accordingly, it can be used to produce recycled cement (RC). This study aimed to evaluate the performance of a solidification agent manufactured using recycled cement (SRC) for the safe packing of radioactive wastes, such as coarse aggregates of CW, waste soil, and metal wastes originating from decommissioned nuclear facilities. The experimental results indicated that the most relevant incineration temperature of CWP for RC was 700 °C. The optimum water-to-binder ratio was determined to be 0.4, and the most relevant substitution ratio of ground granulated blast furnace slag for CWP was determined to be 15%. In addition, calcium silicate hydrate is the most effective hydration product for improving the compressive strength of SRC. The maximum packing capacities of the SRC for coarse aggregates, waste soil, and metal waste, which were simulated as radioactive wastes, were determined to be 30, 5, and 7 wt%, respectively. The results of leaching tests using SRC containing radioactive wastes contaminated with Co, Cs, and Sr indicated that their leachability indices met the acceptance level for disposal. Consequently, the RC composed of CWP can be used as a solidifying agent to safely dispose of radioactive wastes, such as coarse aggregates, waste soil, and metal waste.

Keywords: concrete waste; recycled cement; decommissioned nuclear-power facilities; solidification; radioactive waste; safe disposal

check for updates

Citation: Jeon, J.-H.; Lee, J.-H.; Lee, W.-C.; Lee, S.-W.; Kim, S.-O. Solidification of Radioactive Wastes Using Recycled Cement Originating from Decommissioned Nuclear-Energy Facilities. *Appl. Sci.* **2024**, *14*, 1781. https://doi.org/10.3390/app14051781

Academic Editor: Dino Musmarra

Received: 10 January 2024
Revised: 19 February 2024
Accepted: 20 February 2024
Published: 22 February 2024

Copyright: © 2024 by the authors. Licensee MDPI, Basel, Switzerland. This article is an open access article distributed under the terms and conditions of the Creative Commons Attribution (CC BY) license (https://creativecommons.org/licenses/by/4.0/).

1. Introduction

Superannuated nuclear energy facilities should be decommissioned worldwide; however, these facilities are expected to increase gradually [1]. According to the International Atomic Energy Agency (IAEA), as of February 2023, there were 423 nuclear power plants in operation, 204 facilities were permanently shut down, and the dismantling of 25 facilities was completed [2]. When decommissioning nuclear facilities, hundreds of thousands of tons of waste are generated, and it has become a pending global issue to guarantee technologies for their reduction and recycling [3]. For this reason, advanced countries such as Germany, the USA, Belgium, and Japan have consistently conducted research on the development of treatment technologies for waste generated from nuclear decommissioning facilities [4,5]. In addition, some countries have already secured superior nuclear decommissioning technologies, including decontamination, reduction, and recycling of nuclear waste [6–8].

Nuclear power facilities have reinforced concrete structures, and a considerable amount of waste, such as cementitious waste, coarse and fine aggregates, waste soil, and metal waste, is generated from the process of decommissioning them [9,10]. In addition,

according to a report by the European Commission (EC), 5 million tons of concrete waste (CW) are expected to be generated from the decommissioning process in Europe until 2060 [6]. Most CW is classified as ultralow-level radioactive waste, constituting approximately 60–80% of the total waste [11,12]. Aggregate and cement powder can be separated from CW using thermal and mechanical treatments, and the aggregate is generally fractionated into recycled coarse and fine aggregates based on the size of 5 mm [13]. During the crushing, grinding, and separation processes of CW, powder is generated, which consists of constituents originating from the cement paste as well as fine aggregate [14]. This powder contains many inorganic substances, such as calcium silicate hydrate (CSH), calcium hydroxide (CH), and SiO_2, which are effective materials for waste treatment. Therefore, the powder can be used for recycled cement (RC) after crushing and burning more than twice [15]. Accordingly, instead of disposing of the powder, it is utilized as a solidifying agent for RC, leading to a decrease in the usage of common solidifying agents, such as Portland cement, as well as reducing the amount of waste and cost of disposal [16]. In addition, waste soil is generated from the decommissioning process, and it contains some clay minerals, such as illite and zeolite, which show an excellent capacity for adsorbing radioactive nuclides. Hence, if waste soil can be used as an adsorbent, not only is the amount of radioactive waste reduced, but safe disposal is also ensured [17].

Research on the application of concrete waste powder (CWP) originating from the decommissioning process to RC has been conducted continuously since 2000. However, it remains problematic that it shows insufficient compressive strength and an unbalanced chemical composition due to the constituents originating from fine aggregates [18,19]. Therefore, there is a need to focus on the separation of waste cement powder from fine aggregates. To compensate for this problem, some studies have been conducted to improve the RC quality by blending cementitious waste powder with industrial by-products, such as blast furnace slag (BFS) and fly ash (FA), which are used as cement admixtures (adjusting agents) to increase their compressive strength [20–22]. BFS can improve the compressive strength of RC as a result of the hydration reaction because it has a 30% CaO content and can be used as a substitute for ordinary Portland cement (OPC) [23]. However, BFS exhibits potential hydraulicity (hydraulic properties), and the addition of alkaline reagents is required for hydration [24].

This study was conducted to evaluate the manufacturing process of a solidification agent using recycled cement (SRC) for the safe packing of radioactive wastes, such as coarse aggregates of CW, waste soil, and metal wastes originating from the decommissioning process of nuclear facilities. RC was produced as a replacement for OPC using low-level or ultralow-level radioactive cementitious waste powders. The specific objectives were to (1) determine the optimum mixing ratio of RC, (2) elucidate the manifestation mechanism of compressive strength, (3) assess the maximum packing capacity of SRC for radioactive wastes based on the disposal acceptance criterion of the compressive strength, and (4) evaluate the leachability of SRC according to the types of radioactive waste and radionuclides contained. Because each country has a different regulatory system on the criteria for the safe disposal of radioactive wastes, this study focused on internationally common standards, such as compressive strength and leachability index.

2. Materials and Methods

2.1. Materials

The study was conducted using materials and methods similar to those of Jeon et al. (2023) [25]. As mentioned above, the goal of this study was to manufacture an SRC capable of containing radioactive waste using CW generated by decommissioning. However, it is difficult to bring radioactive CW into the laboratory for experiments. Therefore, CW was simulated by producing the concrete before the experiments and then crushing and grinding it to a size smaller than 0.38 μm. There are various methods for manufacturing commercial concrete mixtures. However, strict requirements for concrete are needed for constructing nuclear power facilities, and internationally accepted guidelines, such as

American Concrete Institute (ACI) 301 and 304, have been used for that. The general ratios of concrete mixtures used for nuclear power facilities are OPC (10–15 wt%), coarse aggregate (40–45 wt%), and fine aggregate (40–50 wt%) [25–27]. In addition, FA is recommended for controlling the heat generated by hydration reactions, and the compressive strength of concrete in nuclear power facilities is 30–45 MPa [28]. The concrete used in this study was prepared using the ratio of OPC (20.8 wt%), fine (38.9 wt%), and coarse (40.3 wt%) aggregates with water-to-binder (W/B) ratio of 0.38 wt% [25]. After 28 days of curing, the compressive strength of the manufactured concrete was measured to be 35 MPa. Ground granulated blast furnace slag (GGBFS), a by-product of the pig iron manufacturing process, was obtained from the Pohang Iron & Steel Company, Pohang, Korea, and was used as an admixture (adjusting agent) to improve the workability of the RC [25]. GGBFS did not exhibit any difference in chemical composition according to its particle size, and it was crushed to the same size as CW to improve its capacity for hydration or pozzolanic reaction. Typical alkaline reagents, such as NaOH, KOH, and $Ca(OH)_2$, were used to enhance hydration reactions [25]. In addition, lime was injected to prevent the quick setting of the RC. CWP underwent the hydration process, and we assessed the optimum incinerating temperature relevant for deriving the rehydration of RC based on the mechanism of pyrolysis [29]. Four temperatures (500 °C, 600 °C, 700 °C, and 800 °C) were evaluated in a laboratory muffle furnace. Coarse aggregates larger than 5 mm are reported to occupy a high proportion of the waste originating from the nuclear decommissioning process, and they were packed within the manufactured SRC before its diverse properties were investigated [8,25]. Stepwise experiments were conducted using coarse aggregates, waste soil, and metal waste to measure the maximum capacity of the SRC to solidify radioactive waste. Soil samples having a particle size smaller than 75 μm were obtained from a site in the vicinity of the Wolsong Nuclear Power Plant, which is one of the operating nuclear power plants in Korea, and they were used to simulate the waste soil [25]. On the contrary, the metal waste belongs to the group of ordinary dismantlement waste, and stainless-steel plate (SUS 304), which is commonly used in the pipeline of nuclear power facilities, was used in the experiments to simulate the metal waste after it was cut into 5 × 5 × 1 mm pieces [25,30]. The maximum capacity of SRC to pack coarse aggregate, waste soil, and metal waste was determined when its compressive strength satisfied the acceptance level (3.44 MPa) required by the disposal sites [25]. First, a series of experiments were conducted to investigate the maximum capacity of SRC to contain coarse aggregates because they account for the largest portion of CW originating from decommissioning nuclear facilities [13,31]. The results indicated that the compressive strength of SRC was acceptable when the coarse aggregate content was 30 wt%. Therefore, the maximum capacity of the SRC to pack waste soil and metal waste was investigated with a fixed ratio (30 wt%) of coarse aggregates, and then, the changes in the leachability of radionuclides and compressive strength were evaluated using the SRC containing waste soil and metal waste [25].

2.2. Leaching Test

Leaching tests on the SRC containing the radioactive wastes were conducted using waste soil and metal waste, which were artificially contaminated with nonradionuclides of Co, Cs, and Sr because it was impossible to bring practical radioactive waste to the laboratory. In addition, nonradionuclides exhibit chemical behaviors similar to radionuclides, and they were used instead of radionuclides [31]. The international method, which was proposed by the American Nuclear Society and coded by ANS 16.1, was used in the leaching tests, and the leachability was computed using Equation (1) [6,32]:

$$L_i = \frac{1}{10} \sum_1^{10} \left[\log\left(\frac{\beta}{D_i} \right) \right] \quad (1)$$

where L_i represents the leachability of the i-th radionuclide. The β and D_i represent the constant with a value of 1.0 cn^3/s and the effective diffusion coefficient of the i-th radionuclide, respectively.

2.3. Mixing Ratios and Curing Methods

The study was conducted with particular objectives: (1) to determine the optimum blending ratio of SRC; (2) to elucidate the manifestation mechanisms of compressive strength; (3) to compare the maximum capacity of SRC to pack radioactive wastes; and (4) to measure the leachability of radionuclides included in radioactive wastes.

First, the optimum blending ratio was determined through experiments designed under different conditions, such as the W/B ratio, burning temperature of the CWP, type of alkaline reagent, amount of adjusting agent (admixture) (GGBFS), and curing method (Table 1). Furthermore, the effect of the curing method type was evaluated by comparing the compressive strengths between four curing methods, such as air-drying, water, atmospheric steam, and high-pressure and high-temperature curing methods [25]. Table 2 shows the conditions of the experiments in detail. Subsequently, CSH and ettringite, which are known to be typical hydration products, were intentionally added to elucidate the manifestation mechanism of compressive strength, and the relative effect of both substances on compressive strength was compared [25]. We evaluated which was more effective in enhancing the strength; the experimental conditions are presented in Table 3. The maximum capacity of the SRC to contain radioactive waste was investigated using coarse aggregates of CW, waste soil, and metal waste, and the detailed experimental conditions are given in Table 4. Finally, those three types of radioactive waste were deliberately contaminated with Co, Cs, and Sr to compare the leachability between the types of radioactive waste and radionuclides [25]. The experimental conditions are listed in Table 5. After 28 days of curing, leachability tests were conducted using ANS 16.1. SRC was manufactured under different conditions, as shown in Tables 3–5. Refer to Jeon et al. (2023) for all the other specific procedures used for producing SRC [25].

2.4. Measurement of Compressive Strength

The effect of different manufacturing conditions on the compressive strength of SRC was compared, and relevant conditions were determined based on whether they satisfied the disposal criterion (3.44 MPa) for disposal [25]. According to the standard methods, such as ASTM C39 and KS F 2405 [33–37], the compressive strength of the SRC was estimated at 7, 14, 21, and 28 days during the one-month curing period following [25]. More details on the experimental methodology are referred to by Jeon et al. (2023) [25].

2.5. Instrumental Analyses

The properties of SRC were investigated using the procedures and methods suggested by Jeon et al. (2023) [25]. X-ray fluorescence (XRF) (S8 TIGER, Bruker AXS, USA) was used to investigate the chemical compositions of the CWP and GGBFS. After the 28-day curing of SRCs, their compressive strength, mineralogical composition, and microstructure were successively investigated. For the examination of mineralogical features of SRC, it was crushed into a size smaller than 74 μm using a ball mill and X-ray diffractometer (XRD) (Siemens (Munich, Germany) D5005, Cu-Kα, 40 kV, 35 mA, step size: 0.02 Deg, Time/step: 5 s) [25]. Furthermore, the microstructure of the SRC was observed using a low-accelerating voltage field-emission scanning electron microscope (SEM) (JSM-7900F, JEOL, Peabody, MA, USA), and the hydration products of the SRC were observed using a Raman spectrometer (Ramantouch, Nanophoton, Osaka, Japan) [25]. The Raman spectrometer was calibrated using a silicon wafer before analysis. The laser having a wavelength of 785 nm was used for Raman analyses to minimize the interference of fluorescent material, and the other conditions were the beam spot of 50 μm, the laser power of 11 mW, and the exposure time of 30 s. To improve the reliability of the Raman analyses, the final results served as the average of the spectra after each sample was measured twenty times at different spots [25].

Table 1. Experimental conditions for determining the optimum blending ratio of materials (unit: weight %).

	Exp. No.	Binder						Simulated Radioactive Waste (Coarse Aggregate >5 mm)	Water/ Binder Ratio	Curing Method
		Concrete Waste (<0.38 μm)	Alkaline Reagent			Adjusting Agent (GGBFS)	Gypsum			
			NaOH	KOH	$Ca(OH)_2$					
Water/ binder ratio	W/B 0.3	67	-	-	-	-	3	30	0.3	Air-drying
	W/B 0.4	67	-	-	-	-	3	30	0.4	
	W/B 0.5	67	-	-	-	-	3	30	0.5	
	W/B 0.6	67	-	-	-	-	3	30	0.6	
Burning temperatures	500 °C	67	-	-	-	-	3	30	0.4	Air-drying
	600 °C	67	-	-	-	-	3	30	0.4	
	700 °C	67	-	-	-	-	3	30	0.4	
	800 °C	67	-	-	-	-	3	30	0.4	
Mixing ratio of GGBFS	WC-1	57	5	-	-	5	3	30	0.4	Air-drying
	WC-2	52	5	-	-	10	3	30	0.4	
	WC-3	47	5	-	-	15	3	30	0.4	
	WC-4	42	5	-	-	20	3	30	0.4	
Type of alkaline reagents	NaOH	47	5	-	-	15	3	30	0.4	Air-drying
	KOH	47	-	5	-	15	3	30	0.4	
	$Ca(OH)_2$	47	-	-	5	15	3	30	0.4	
Curing method	Air-drying	47	-	-	5	15	3	30	0.4	Air-drying
	Water	47	-	-	5	15	3	30	0.4	Water
	Atmospheric steam	47	-	-	5	15	3	30	0.4	Atmospheric steam
	High pressure and high temperature	47	-	-	5	15	3	30	0.4	High pressure and high temperature

Table 2. Conditions of different curing methods.

Method	In the Mold with a Size of 27 × 27 × 54 mm		Demolded	
	Condition	**Period (Hour)**	**Condition**	**Period (Day)**
Air-drying	In a room environment (20 °C, and 50% relative humidity)	24	In a room environment (20 °C and 50% relative humidity)	28
Water	In a room environment (20 °C and 50% relative humidity)	24	In a water tank (20 ± 2 °C)	28
Atmospheric steam	In a room environment (20 °C and 50% relative humidity) Gradually increased at a rate of 15 °C/h Maintained at 65 °C	2 4 6	After natural cooling, in a room environment (20 °C and 50% relative humidity)	28
High pressure and high temperature	In a room environment (20 °C and 50% relative humidity) 10 atm, gradually increased at a rate of 90 °C/h 10 atm, maintained at 180 °C Under the pressure of 10 atm, gradually decreased at a rate of 90 °C/h until reached 20 °C	4 2 7 2	In a room environment (20 °C and 50% relative humidity)	28

Table 3. Experimental conditions for elucidating the manifestation mechanisms of compressive strength (unit: weight %).

Exp. No.	Binder						Simulated Radioactive Waste (Coarse Aggregate >5 mm)	Water/ Binder Ratio	Curing Method
	Concrete Waste (<0.38 μm)	**CSH**	**Ettringite**	**Alkaline Reagent [$Ca(OH)_2$]**	**Adjusting Agent (GGBFS)**	**Gypsum**			
RC-1	47	-	-	5	GGBFS	3	30	0.4	Air-drying
RC-2	44.5	2.5	-	5	15	3	30	0.4	
RC-3	42	5	-	5	15	3	30	0.4	
RC-4	44.5	-	2.5	5	15	3	30	0.4	
RC-5	42	-	5	5	15	3	30	0.4	
RC-6	44.5	1.25	1.25	5	15	3	30	0.4	
RC-7	42	2.5	2.5	5	15	3	30	0.4	

Table 4. Experimental conditions for determining the maximum capacity of SRC to contain radioactive wastes (unit: weight %).

Exp. No.	Binder				Simulated Radioactive Waste			Water/ Binder Ratio	Curing Method
	Concrete Waste (<0.38 μm)	Alkaline Reagent [$Ca(OH)_2$]	Adjusting Agent (GGBFS)	Gypsum	Coarse Aggregate (>5 mm)	Waste Soil (<0.75 mm)	Metal Waste		
CWS-1	51	5	10	3	30	1	-	0.4	Air-drying
CWS-2	50	5	10	3	30	2	-	0.4	
CWS-3	49	5	10	3	30	3	-	0.4	
CWS-4	48	5	10	3	30	4	-	0.4	
CWS-5	47	5	10	3	30	5	-	0.4	
CWS-6	46	5	10	3	30	6	-	0.4	
CWS-7	45	5	10	3	30	7	-	0.4	
CM-1	51	5	10	3	30	-	1	0.4	
CM-2	50	5	10	3	30	-	2	0.4	
CM-3	49	5	10	3	30	-	3	0.4	
CM-4	48	5	10	3	30	-	4	0.4	
CM-5	47	5	10	3	30	-	5	0.4	
CM-6	46	5	10	3	30	-	6	0.4	
CM-7	45	5	10	3	30	-	7	0.4	
CM-8	44	5	10	3	30	-	8	0.4	

Table 5. Experimental conditions for determining the leachability of each radionuclide contained in different radioactive wastes (unit: weight %).

	Binder				Simulated Radioactive Waste			Water/ Binder Ratio	Radionuclide Concentration (mg/L)			Curing Method
	Concrete Waste (<0.38 μm)	Alkaline Reagent [$Ca(OH)_2$]	Adjusting Agent (GGBFS)	Gypsum	Coarse Aggregate (>5 mm)	Waste Soil (<0.75 mm)	Metal Waste		Co	Cs	Sr	
Co	47	5	10	3	30	-	5	0.4	538	-	-	Air-drying
Cs	47	5	10	3	30	-	5	0.4	-	347	-	
Sr	47	5	10	3	30	-	5	0.4	-	-	487	
Co-1	47	5	10	3	30	5	-	0.4	21,255	-	-	
Co-2	47	5	10	3	30	5	-	0.4	23,622	-	-	
Co-3	47	5	10	3	30	5	-	0.4	25,988	-	-	
Cs-1	47	5	10	3	30	5	-	0.4	-	8868	-	
Cs-2	47	5	10	3	30	5	-	0.4	-	9863	-	
Cs-3	47	5	10	3	30	5	-	0.4	-	10,843	-	
Sr-1	47	5	10	3	30	5	-	0.4	-	-	15,406	
Sr-2	47	5	10	3	30	5	-	0.4	-	-	17,138	
Sr-3	47	5	10	3	30	5	-	0.4	-	-	18,842	

3. Results and Discussions

3.1. Properties of Materials

The XRF results for the chemical compositions of the CWP and GGBFS are given in Table 6. Compared with the OPC showing SiO_2 (21–43%) and CaO (51–63%) contents [38,39], the contents of the CWP were measured to be approximately 45% and 19%, respectively, and the relatively higher SiO_2 and lower CaO contents indicated that a significant proportion of powder was likely to originate from fine aggregate rather than cementitious waste during the crushing, grinding, and separation processes for the pretreatment of CW. GGBFS exhibited a larger content of CaO (approximately 37%) and seemed relevant for use as an admixture (adjusting agent).

Table 6. The XRF results on the chemical compositions of the CWP and GGBFS (unit: weight %).

	SiO_2	CaO	Al_2O_3	Fe_2O_3	K_2O	Na_2O_3	MgO	SO_3	Others	LOI
Concrete waste (<0.38 μm)	44.5	18.8	8.73	3.36	1.9	1.82	1.66	0.99	1.07	17.16
GGBFS	32	36.8	13.7	0.55	-	0.53	3.39	1.25	2.24	9.54

The effect of burning temperature on the mineralogical composition of CWP was investigated using XRD, and the results are shown in Figure 1. Usually, the peaks of CH are known to be strong in hardened cement paste as a result of hydration, but those of β-C_2S (β-belite) are not likely to be detected because CH is consumed by the process of hydration [6,21]. However, the peaks corresponding to the CH were not observed at the burning temperatures of control (room temperature), 500 °C, and 600 °C, which is attributed to its transformation to calcite due to the mediation of CO_2. At burning temperatures over 700 °C, the calcite peaks were weakened, and those of β-C_2S appeared due to the decarboxylation of calcite [21,40]. Consequently, the results suggest that CWP should be burned at temperatures over 700 °C for use in RC. Furthermore, 700 °C was determined to be the optimum burning temperature because the intensity of the β-belite peaks did not increase above 700 °C. Therefore, the burning temperature was set to be 700 °C for the other experiments. Constituents, such as C_3S and β-C_2S, are required for the hydration reaction of cement. C_3S and β-C_2S are known to form when Ca and Si contents are high, respectively [41]. β-C_2S was the focus of this study because the Si content appeared to be comparatively higher owing to the mingling of the fine aggregate constituent, as mentioned above. The effect of burning temperature on the compressive strength of the SRC was investigated, and the results are shown in Figure 2. After 28 days of curing, the results of burning temperatures up to 600 °C did not meet the disposal standard of compressive strength, but those above 700 °C satisfied the criterion. These results indicate that the compressive strength of the RC improved because of the CSH produced from the hydration reaction of β-C_2S.

3.2. Optimum Mixing Ratio

3.2.1. Water-to-Binder Ratio

The water-to-binder (W/B) ratio influences the workability, strength, and durability of SRC, and it should be optimized [25]. The variations in the compressive strength of SRC were investigated for different W/B ratios and curing periods (Figure 3). The SRC showed compressive strength meeting the disposal criterion (3.44 MPa) when the W/B ratios were 0.3 and 0.4 after 28 days of curing. In the cases of 0.5 and 0.6 W/B ratios, the compressive strengths of SRC were measured to be 3.1 and 2.8 MPa, respectively, after the same period of curing, and they did not satisfy the disposal standard. Compared with OPC, CWP contained an insufficient quantity of substances, such as β-C_2S, which could provoke the hydration reaction. Therefore, the compressive strength of the SRC was weakened with W/B ratios greater than 0.5 because the water was likely to exceed the quantity needed for

the hydration reaction, and the surplus water was likely to form capillary pores rather than facilitate the reaction. Consequently, based on the results, a W/B ratio of 0.4 seemed to be the optimum level for meeting the criterion and improving workability.

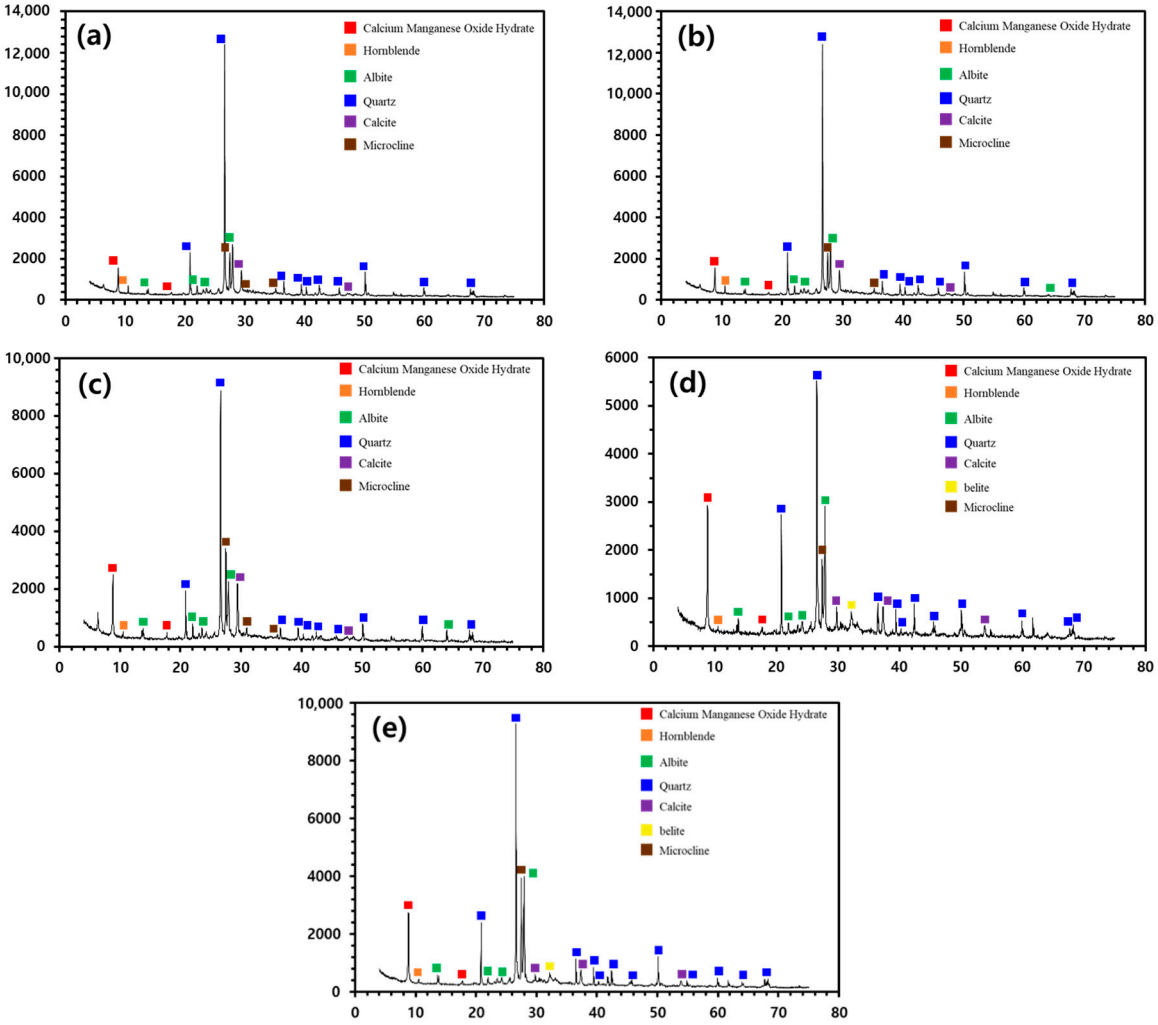

Figure 1. The effect of burning temperatures on the mineralogical composition of the CWP. (**a**) Control (room temperature), (**b**) 500 °C, (**c**) 600 °C, (**d**) 700 °C, and (**e**) 800 °C.

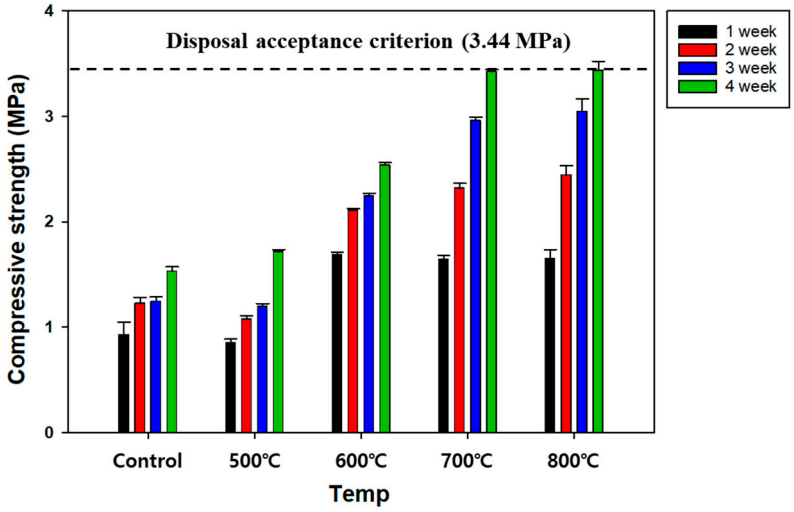

Figure 2. The effect of burning temperatures on the compressive strength of the SRC.

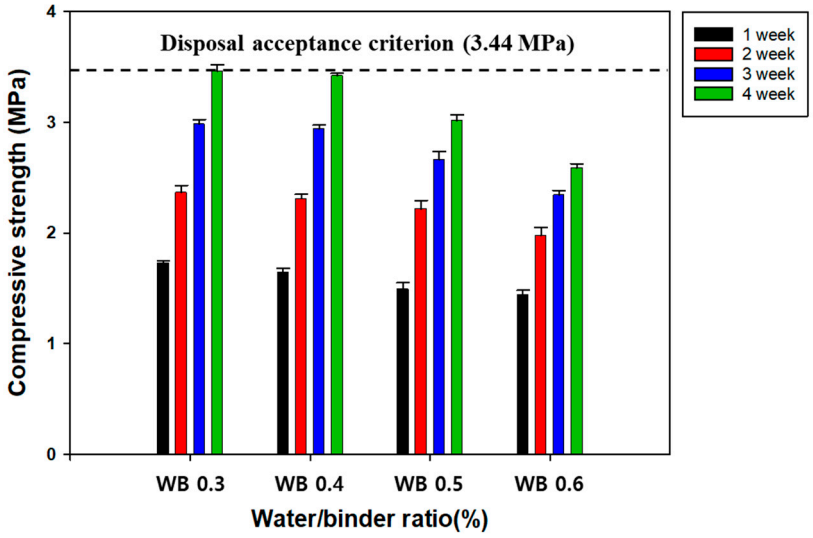

Figure 3. The effect of W/B ratios on the compressive strength of the SRC.

3.2.2. Mixing Ratio of GGBFS

RC manufactured using CWP as a replacement material for OPC could show some defects, such as a relatively lower Ca content as a result of the mingling of fine aggregate constituents and a decrease in strength. Compared with OPC, CWP experienced the burning process, and the RC using it exhibited remarkably lower contents of hydration-provoking materials, such as β-C_2S. Therefore, industrial by-products containing a relatively higher Ca content, such as FA and GGBFS, were added to supplement the insufficient CaO content of CWP and improve the quality of RC. In this study, the effect of GGBFS on the compressive strength of SRC was investigated, and the results are presented in Figure 4. Overall, the compressive strength of the SRC increased with increasing GGBFS content. Specifically, the disposal criterion was met with GGBFS contents of over 15% after 28 days of curing, as shown in the cases of WC-3 and WC-4 in Figure 4. Therefore, the optimal GGBFS substitution ratio for CWP was determined to be 15%.

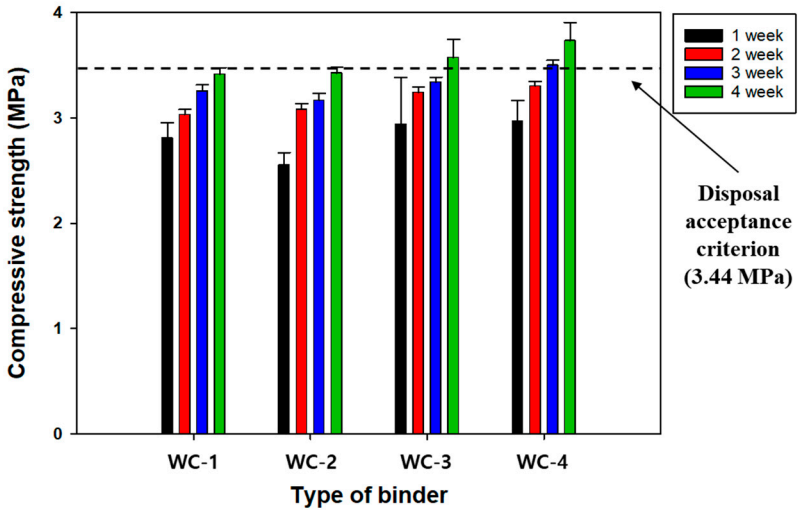

Figure 4. The effect of GGBFS contents on the compressive strength of SRC. Refer to the detailed experimental conditions in Table 1.

3.2.3. Types of Alkaline Reagents

GGBFS is potentially hydraulic, i.e., it is not water-soluble, and introducing alkaline reagents is needed to stimulate its surface and promote the hydration reaction [25]. Alkaline reagents can eliminate the film on the GGBFS surface and dissolve its chemical constituents.

Accordingly, dissolved ions, such as Ca, generate hydration products, increasing SRC's compressive strength [25]. NaOH, KOH, and $Ca(OH)_2$ are the most frequently used alkaline reagents; however, few studies have shown their performance. Therefore, the effects of different alkaline reagents on the compressive strength of SRC were investigated (Figure 5). After 28 days of curing, the compressive strength increased in the order $Ca(OH)_2$ > KOH > NaOH. In particular, the compressive strengths of KOH and $Ca(OH)_2$ were measured to be 4 MPa immediately after only 7 days of curing and met the disposal criteria. According to Park et al. (2013), NaOH and KOH were likely to effectively catalyze the stimulation of the surface of GGBFS, but $Ca(OH)_2$ prevented hydration products, such as CSH, from forming due to the consumption of Si by Ca [42]. On the contrary, Li et al. (2022) reported that $Ca(OH)_2$ could enhance the compressive strength of RC because the efficient interaction of Ca with SiO_2 and Al_2O_3 improved the formation of hydration products, such as CSH and calcium aluminate hydrates (CAH) [43]. These results confirmed that the interaction of Ca with SiO_2 formed CSH and finally improved the compressive strength.

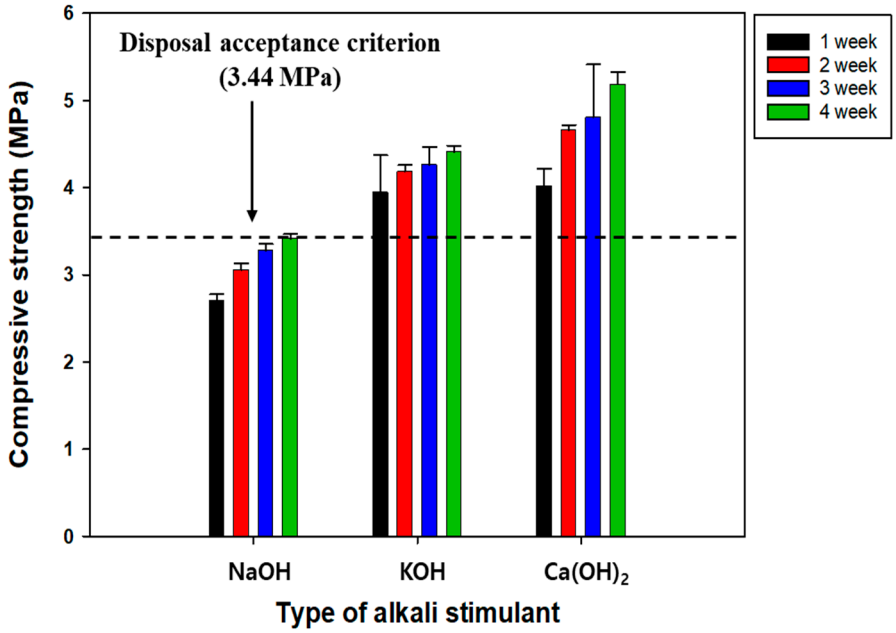

Figure 5. The effect of different types of alkaline reagents on the compressive strength of SRC.

3.3. Effect of Curing Methods on the Compressive Strength of SRC

Typically, SRC exhibits a much lower compressive strength than OPC-based concrete, and it is necessary to improve it using effective curing methods. Four commonly used curing methods (air-drying, water, atmospheric steam, and high-pressure and high-temperature curing methods) were compared to reveal their effect on the compressive strength of SRC (Figure 6) [25]. The results showed that the increasing sequence of compressive strength was water > high-pressure and high-temperature > air-drying > atmospheric steam, and all curing methods satisfied the disposal criterion. On the other hand, the air-drying, atmospheric steam, and high-pressure and high-temperature curing methods showed relatively lower compressive strengths, which was attributed to an insufficient hydration reaction due to the evaporation of water. Meanwhile, in terms of the water curing method, hydration products, such as CSH and ettringite ($Ca_6Al_2(SO_4)_3(OH)_{12}\cdot 26H_2O$), were continuously formed, increasing the compressive strength [25]. The experimental results showed that the best curing method was water curing, based on the disposal criterion of compressive strength. However, the air-drying curing method seems more relevant when considering the disposal standard, cost-effectiveness, and convenience [25].

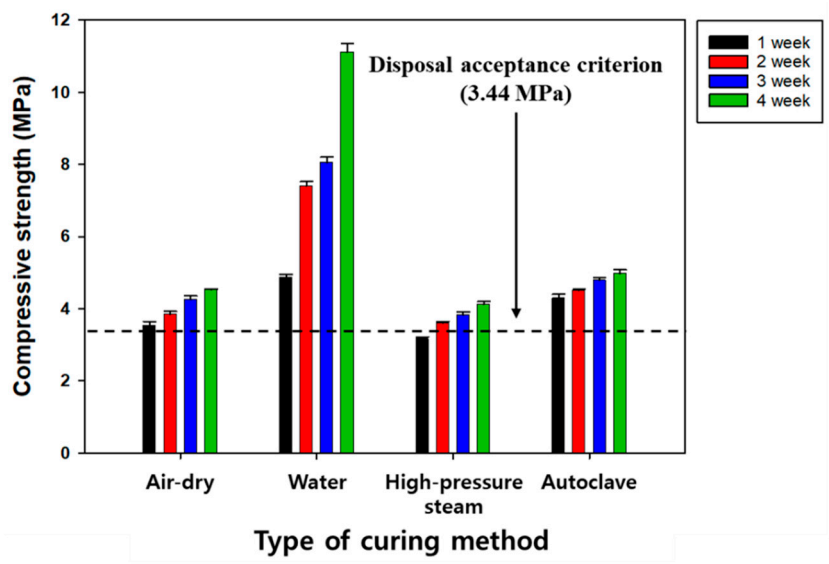

Figure 6. The effect of curing methods on the compressive strength of SRC.

3.4. Manifestation Mechanism of Compressive Strength

Ettringite, CSH, CH, and unhydrated clinker grains are known to be representative products of the hydration reaction occurring in cement [41]. Ettringite is a chemical compound of needle-like crystals that improves the initial strength of cement and is finally transformed into monosulfate [$Ca_4Al_2O_6(SO_4)\cdot 12H_2O$] of sheet-like hexagonal crystals [44–46]. Meanwhile, CSH is reported to have a colloidal size and significantly affects the strength of cement [46]. CH exists as sheet-like hexagonal crystals and has a minor impact on the strength of cement because it has a relatively smaller specific surface area than CSH [47]. In addition, CH is less chemically stable because of its higher solubility [47,48]. However, few studies have examined the initial or long-term effects of hydration products, such as CSH and ettringite, on compressive strength [25]. Accordingly, CSH and ettringite were deliberately introduced to investigate which was more effective in improving the compressive strength of SRC, and the results are given in Figure 7. The compressive strengths were enhanced by the introduction of hydration products and met the disposal standard only after 7 days of curing when adding hydration products. Moreover, the results indicate that CSH was more effective than ettringite in improving compressive strength [25]. The microstructure of SRC was investigated using SEM to investigate the manifestation mechanism of the compressive strength of both materials. Three different types of SRC were manufactured for SEM analyses: (1) with neither substance, (2) with the addition of 5% CSH, and (3) with the addition of 5% ettringite, and the results are shown in Figure 8. Without either material, needle-like ettringites were observed above the sheet-like CH, gel-shaped CSHs, and some pores. In the second case, gel-shaped CSHs were predominant, and most of the pores were filled with CSHs, compared with the first case. The last case exhibited net-like structures with mixtures of sheet-like CH, gel-shaped CSHs, and ettringite-blocked pores. The order of none of the materials > ettringite > CSH tended to increase the pore volume, and the opposite tendency was observed in the compressive strength values [25]. Therefore, the CSH exhibited a relatively higher contribution to improving compressive strength than ettringite because the former was gel-shaped and effectively blocked the inner pore spaces of SRC. Their Raman spectra were obtained to examine the effect of the hydration products on the compressive strength of SRC more closely (Figure 9). The results indicated that the peaks corresponding to CSH and ettringite were observed at 650 and 960 cm^{-1}, respectively, for all the cases tested, and also the spectra of CH and $CaCO_3$ were obtained [25]. Without adding both substances (Figure 9a), the width and intensity of the CSH peak appeared to be narrower and higher than those of ettringite, respectively, indicating the higher crystallinity of CSH than ettringite. In addition, identical results were acquired when both substances were added at equivalent amounts (5 wt%)

(Figure 9b,c). These results were consistent with the measurement results of the compressive strength of SRC, and the more significant contribution of CSH to the compressive strength of SRC might be due to its higher crystallinity.

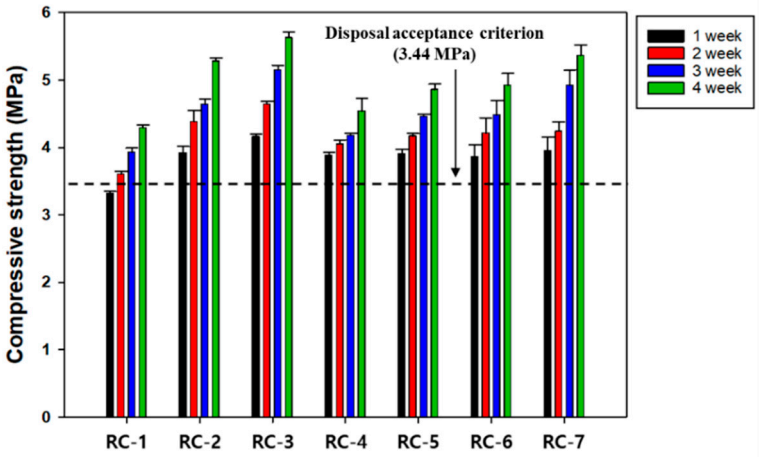

Figure 7. The effect of different types of hydration products on the compressive strength of SRC. Refer to the detailed experimental conditions in Table 3.

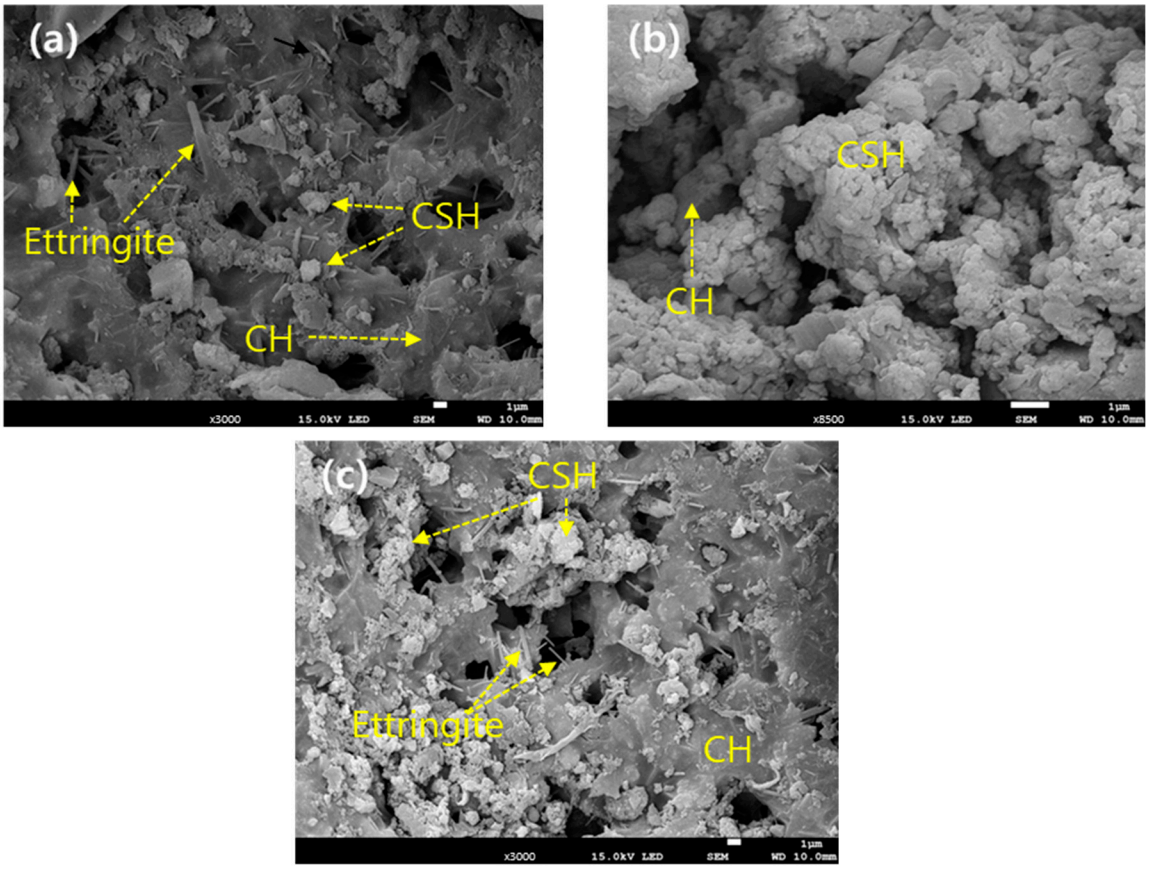

Figure 8. The SEM results on the microstructure of SRC. (**a**) Without the addition of CSH and ettringite, (**b**) with the addition of CSH (5 wt%), and (**c**) with the addition of ettringite (5 wt%).

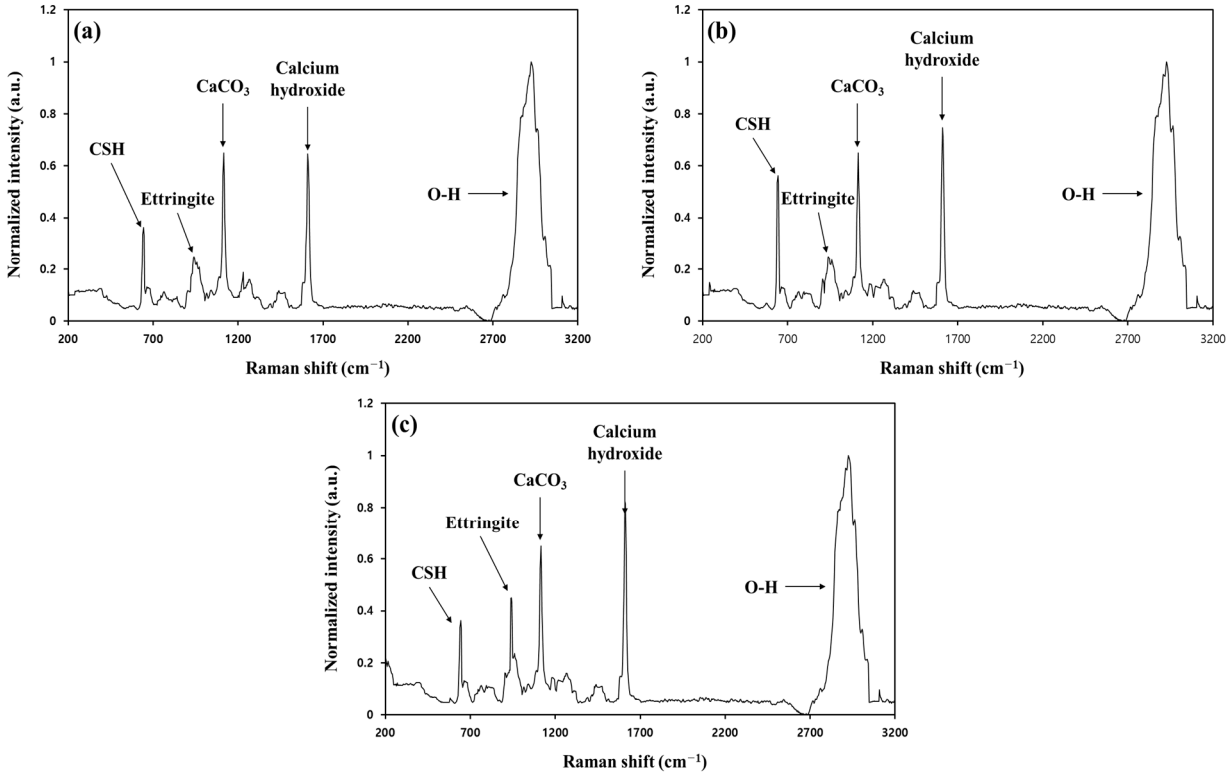

Figure 9. The Raman spectra. (**a**) Without the addition of CSH and ettringite, (**b**) with the addition of CSH (5 wt%), and (**c**) with the addition of ettringite (5 wt%).

3.5. Simulation of the Solidification of Radioactive Wastes Using SRC

A massive amount of solid waste, such as CW, waste soil, and metal waste, originates from the decommissioning process of nuclear power facilities, and that type of waste affects the compressive strength of SRC [25]. For this reason, the changing tendency of SRC's compressive strength was investigated according to the type of waste, and its maximum capacity for packing the waste was determined. As the coarse aggregate of CW occupies the highest proportion of the solid waste occurring from the dismantling process, the maximum capacity of SRC containing CW was first investigated [25]. The results showed that 30 wt% was the maximum proportion of coarse aggregates packed in SRC. Then, the maximum solidifying capacities of SRC for waste soil and metal waste were evaluated using a fixed ratio (30 wt%) of coarse aggregates. Moreover, because experiments were impossible using practical radioactive nuclides, their leachability was indirectly assessed using nonradionuclides, such as Co, Cs, and Sr, which were intentionally introduced into each waste. Before the experiments on the leachability of waste soil, the maximum adsorption capacities of the nonradionuclides were empirically determined to choose their relevant spiking levels [25], and the maximum adsorbed concentrations (MAC) of Co, Cs, and Sr were estimated as 23,622, 9863, and 17,138 mg/kg, respectively. The nonradionuclides were injected at three different levels (<10% MAC, equal to MAC, and >10% MAC) [25]. On the other hand, with regard to metal waste, the MAC of each nuclide could not be determined using an identical experimental procedure, and instead, it was sufficiently soaked for 24 h in a solution containing them at a concentration of 50,000 mg/L before the leachability tests [25]. A standard method (ANS 16.1) was used for the leachability tests, and the concentrations of each nuclide were analyzed whenever the leaching solutions were replaced during the total period of 90 days. Finally, their leachabilities were calculated using Equation (1). Whether each waste type was suitable or not was evaluated by comparing their leaching indices based on the acceptance level of 6. The SRC's compressive strength was also analyzed again following the leaching tests.

3.5.1. Maximum Packing Capacity of SRC for Radioactive Wastes

The maximum packing capacities for the waste soil and metal waste are shown in Figure 10. As expected, the solidification of the coarse aggregate and metal waste resulted in a higher compressive strength than that of the coarse aggregate and waste soil. The compressive strength of SRC containing waste soil (5 wt%) and coarse aggregate (30 wt%) was investigated to meet the disposal criterion after 28 days of curing. In contrast, 7 wt% metal waste and 30 wt% coarse aggregate exhibited compressive strengths that satisfied the standard. However, the compressive strength decreased with an increasing portion of metal waste from those higher than 5 wt%, which is likely attributed to its weak binding capacity with SRC and the formation of pore spaces due to the excessive amount of metal waste. Therefore, a suitable packing amount of metal waste of 5 wt% is recommended, even though 7 wt% satisfied the compressive strength criterion.

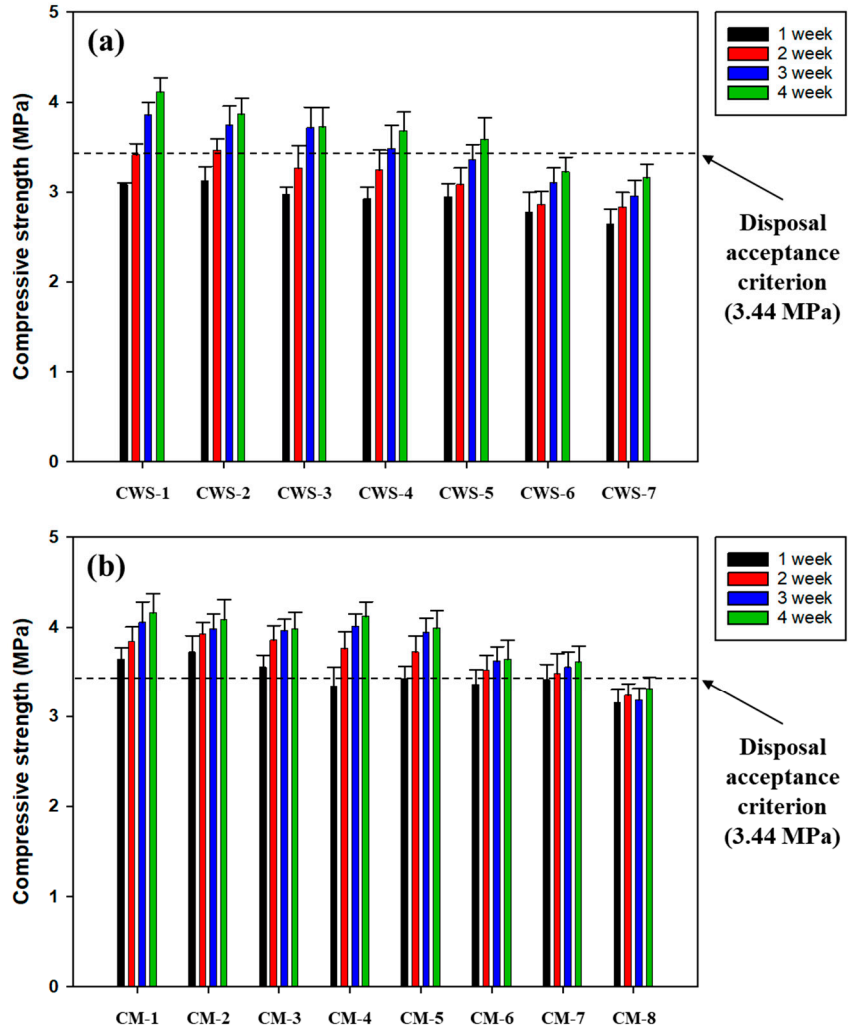

Figure 10. The maximum packing capacities of SRC for the simulated radioactive wastes. (**a**) The case of coarse aggregate and waste soil and (**b**) the case of coarse aggregate and metal waste. Refer to the detailed experimental conditions in Table 4.

3.5.2. Leachability of Radionuclides Contained in Radioactive Wastes

Based on the results of the maximum packing capacity of the SRC, the amounts of each waste used for the leachability tests were 30 wt% for coarse aggregates and 5 wt% for waste soil and metal waste. The leaching indices of each nuclide are given in Table 7, and all values met the acceptance level (6) for disposal. In the case of waste soil, the leaching indices decreased with increasing amounts of spiking, but satisfied the criterion. However, the

leachability indices of waste soil and metal waste at high concentrations tended to increase dramatically, and it is speculated that they could not meet the disposal criterion if the concentration exceeded the levels of this study. Recently, there has been a lot of research to improve the adsorption of radioactive nuclides. Wang et al. (2024) reported that zirconium phosphate(ZrP) is an excellent inorganic adsorbent for radioactive Cs [49], and Zhuang et al. (2023) revealed the predominant affinity of carboxyl-functionalized carbon nanotubes (cCNTs) for radioactive Co as well as their high thermal stability [50]. A comparison of the compressive strength of SRC during the curing period and after the leaching tests is shown in Figure 11. In the case of SRC containing waste soil, its compressive strength was found to be 4.2 MPa and met the standard after 28 days of curing, regardless of the type of nuclide. The case of metal waste showed an acceptable level of compressive strength (4.5 MPa) for all types of nuclides after 28 days of curing. In addition, it was confirmed that the compressive strength of SRC did not change after the 90-day leaching tests in all the cases. Consequently, the results indicated that SRC can be used to safely solidify a considerable amount of radioactive waste contaminated with different radionuclides.

Table 7. The leaching indices of each radionuclide.

	Co	Cs	Sr	Co-1	Co-2	Co-3	Cs-1	Cs-2	Cs-3	Sr-1	Sr-2	Sr-3
Leachability index	14.69	13.96	7.75	14.59	14.16	6.3	14.78	13.84	6.57	14.9	13.13	6.14

Refer to the experimental conditions in Table 5.

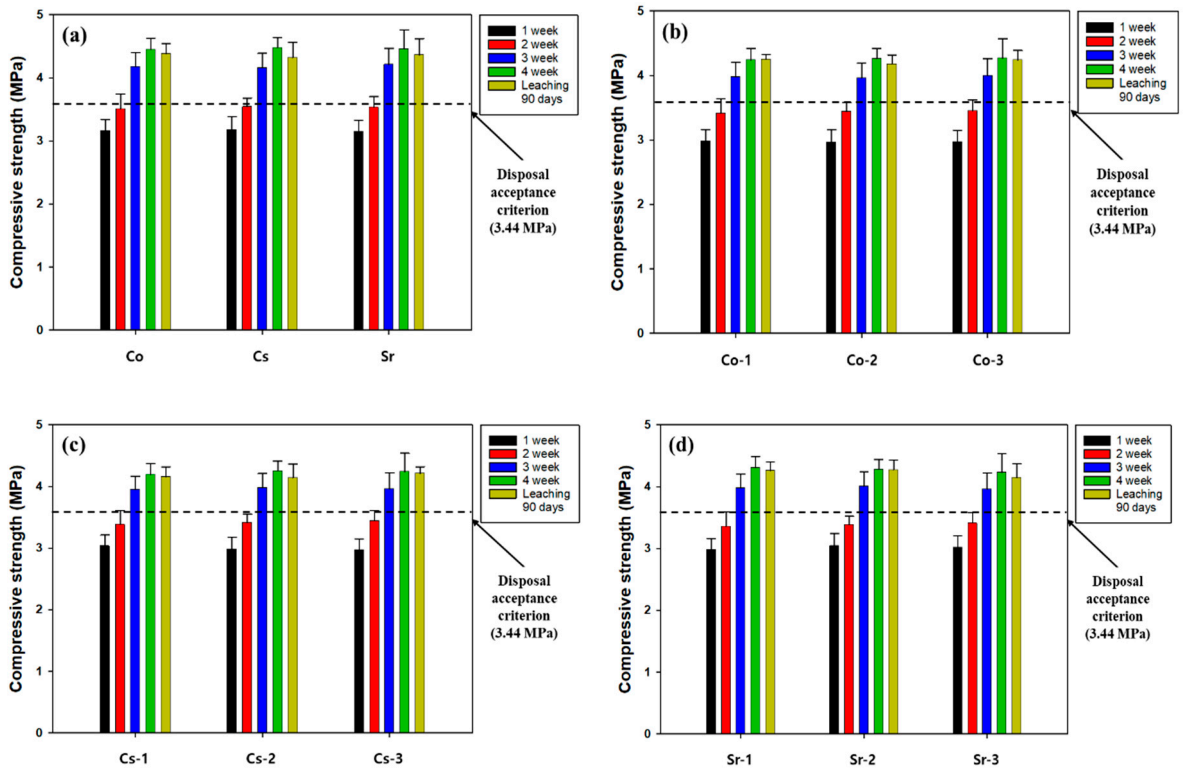

Figure 11. The comparison of the compressive strengths of SRC during the curing period and after leaching test. (**a**) The case of metal waste soaked in the solutions of Co, Cs, and Sr and the cases of waste soil spiked by (**b**) Co, (**c**) Cs, and (**d**) Sr. The numbers 1, 2, and 3 denote three different levels of concentration, which are 10 % lower than maximum adsorption capacity (MAC), equal to MAC, and 10% higher than MAC, respectively. Refer to the detailed experimental conditions in Table 5.

4. Conclusions

This study evaluated the applicability of RC manufactured using ultralow-level radioactive CWP generated from decommissioned nuclear power facilities as a solidifying agent to safely dispose of radioactive wastes, such as coarse aggregates, waste soil, and metal waste, which are considered the most common and above-medium-level radioactive wastes. Specifically, the optimum mixing ratio of materials, manifestation mechanism of compressive strength, maximum packing capacity of SRC for radioactive wastes, and leachability of SRC were assessed. The following conclusions were drawn:

(1) The XRF results for the chemical compositions of CWP and GGBFS showed SiO_2 and CaO contents of 45% and 19%, respectively. The relatively higher SiO_2 and lower CaO contents indicated that a significant proportion of the powder likely originated from fine aggregates rather than cementitious waste during the crushing, grinding, and separation processes for the pretreatment of CW. However, GGBFS exhibited a more significant CaO content (approximately 37%) and seemed relevant for use as an admixture (adjusting agent) to improve the compressive strength of SRC.

(2) The XRD results according to the burning temperatures of CWP indicated that the peaks of β-belite, which are required for the hydration reaction of cement, were not detected at 0–600 °C, but were identified above 700 °C. Furthermore, the compressive strength of the SRC met the disposal criterion at incineration temperatures above 700 °C. Consequently, 700 °C was found to be the most appropriate incineration temperature for the manufacture of the RC.

(3) SRC showed the highest compressive strength when the water-to-binder ratio was 0.4, the GGBFS content was 15 wt%, and CH was used as an alkaline reagent. Among the curing methods tested, the water curing method showed the highest compressive strength (11 MPa) after 28 days of curing. The other methods yielded a compressive strength of 4 MPa and satisfied disposal criteria.

(4) Based on the experimental results to elucidate the manifestation mechanism of the compressive strength, CSH was more effective than ettringite in improving the compressive strength of SRC. The SEM results of the microstructure of SRC revealed that ettringite with needle-like crystals could not fill all the pores of SRC; however, gel-shaped CSH effectively filled the pore space by enclosing calcium hydrate and ettringite. In addition, the analytical results of the Raman spectroscopy indicated that the crystallinity of CSH was higher than ettringite, which supports the more significant contribution of CSH than ettringite to the compressive strength of SRC.

(5) The total maximum packing capacities of the SRC for coarse aggregate, waste soil, and metal waste were determined to be 30, 5, and 7 wt%, respectively, satisfying the disposal criterion for compressive strength. The results of the leaching tests on the simulated radionuclides, such as Co, Cs, and Sr, met the leachability standards for disposal. Furthermore, the compressive strength of SRC met its criterion after 90-day leaching tests.

Overall, this study showed that the radioactive wastes at low and intermediate levels can be safely disposed of by using CW and GGBFS as replacements for OPC. In terms of the industrialization of this process, Oh et al. (2021) proved its feasibility using stepwise experiments on the thermomechanical treatment of radioactive concrete waste [51].

Author Contributions: Conceptualization, S.-O.K.; methodology, J.-H.J. and S.-O.K.; validation, W.-C.L. and S.-W.L.; formal analysis, J.-H.J. and J.-H.L.; investigation, J.-H.J. and J.-H.L.; data curation, W.-C.L. and S.-W.L.; writing—original draft preparation, J.-H.J.; writing—review and editing, S.-O.K.; supervision, S.-O.K.; project administration, S.-W.L.; funding acquisition, S.-O.K. All authors have read and agreed to the published version of the manuscript.

Funding: This work was supported by the Korea Institute of Energy Technology Evaluation and Planning (KETEP) and the Ministry of Trade, Industry & Energy (MOTIE) of the Republic of Korea (RS-2023-00246054).

Institutional Review Board Statement: Not applicable.

Informed Consent Statement: Not applicable.

Data Availability Statement: Data are contained within the article.

Conflicts of Interest: Authors Woo-Chun Lee and Sang-Woo Lee were employed by the company Hosung Inc. The remaining authors declare that the research was conducted in the absence of any commercial or financial relationships that could be construed as a potential conflict of interest.

References

1. Shin, J.S.; Oh, S.Y.; Park, S.K.; Park, H.M.; Kim, T.S.; Lee, L.; Kim, Y.H.; Lee, J.H. Underwater laser cutting of stainless steel up to 100 mm thick for dismantling application in nuclear power plant. *Ann. Nucl. Energy* **2020**, *147*, 107655. [CrossRef]
2. International Atomic Energy Agency (IAEA). The Database on Nuclear Power Reactors, Power Reactor Information System. Available online: https://pris.iaea.org/PRIS/home.aspx (accessed on 5 November 2023).
3. Han, S.S.; Hong, S.J.; Nam, S.S.; Kim, W.S.; Um, W.Y. Decontamination of concrete waste from nuclear power plant decommissioning in south korea. *Ann. Nucl. Energy* **2020**, *149*, 107795. [CrossRef]
4. Volk, R.; Hübner, F.; Schultmann, F. The future of nuclear decommissioning-A worldwide market potential study. *Energy Policy* **2019**, *124*, 226–261. [CrossRef]
5. Lim, Y.J.; Lee, B.S.; Park, S.O.; Lee, S.G. A study on the clearance waste recycling scenario in the decommissioning of Korea's nuclear power plant. *Ann. Nucl. Energy* **2022**, *178*, 109366. [CrossRef]
6. Min, B.Y.; Choi, W.K.; Lee, K.W.; Park, J.W. Evaluation of the compressive strength and leachability for cemented waste using radioactive fine powder. *J. Nucl. Fuel Cycle Waste Technol.* **2009**, *26*, 658–666.
7. Singh, B.K.; Hafeez, M.A.; Kim, H.J.; Hong, S.J.; Kang, J.E.; Um, W.Y. Inorganic waste forms for efficient immobilization of radionuclides. *ACS EST Eng.* **2021**, *1*, 1149–1170. [CrossRef]
8. Chang, I.G.; Cheong, J.H. A new proposal for controlled recycling of decommissioning concrete waste as part of engineered barriers of radioactive waste repository and related comprehensive safety assessment. *Nucl. Eng. Technol.* **2022**, *55*, 530–545. [CrossRef]
9. Oskolkov, B.Y.; Bondarkov, M.D.; Ziinkevich, L.I.; Proskura, N.I.; Farfán, E.B.; Jannik, G.T. Radioactive waste management in the Chernobyl exclusion zone: 25 years since the Chernobyl nuclear power plant accident. *Health Phys.* **2011**, *101*, 431–441. [CrossRef]
10. Moon, J.K.; Kim, S.B.; Choi, W.J.; Choi, B.S.; Chung, D.Y.; Seo, B.K. The status and prospect of decommissioning technology development at KAERI. *J. Nucl. Fuel Cycle Waste Technol.* **2019**, *17*, 139–165. [CrossRef]
11. Poškas, P.; Kilda, R.; Šimonis, A.; Jouhara, H.; Poškas, R. Disposal of very low-level radioactive waste: Lithuanian case on the approach and long-term safety aspects. *Sci. Total Environ.* **2019**, *667*, 464–474. [CrossRef]
12. Son, J.H.; Kong, T.Y.; Yang, H.Y.; Kim, S.J.; Lee, E.J.; Choi, W.S. Estimation of radiation dose resulting from the recycling of large metal wastes from decommissioning nuclear power plants in korea. *Energy Sci. Eng.* **2021**, *9*, 2206–2214. [CrossRef]
13. Cheon, J.H.; Lee, S.C.; Kim, C.L.; Park, H.G. Feasibility study on recycling of concrete waste from NPP decommissioning. *J. Korean Recycl. Constr. Resour. Inst.* **2018**, *6*, 115–122.
14. Kim, J.H.; Seo, E.A.; Kim, D.G.; Chung, C.W. The effect of changes in the separation process for the performance of recycled cement powder: A comparison with a previous study for radioactive waste immobilization. *Materials* **2022**, *15*, 7972. [CrossRef]
15. Bogas, J.A.; Carrico, A.; Tenza-Abril, A.J. Microstructure of thermoactivated recycled cement pastes. *Cement Concr. Res.* **2020**, *138*, 106226. [CrossRef]
16. Heo, Y.Y.; Lee, C.W.; Kim, H.R.; Lee, S.J. Framework for the development of guidelines for nuclear power plant decommissioning workers based on risk information. *Nucl. Eng. Des.* **2022**, *387*, 111624. [CrossRef]
17. Cheon, K.H.; Choi, J.H.; Shin, W.S.; Choi, S.J. Adsorption characteristics of cobalt, strontium, and cesium on natural soil and kaolin. *J. Environ. Sci. Int.* **2014**, *23*, 1609–1618. [CrossRef]
18. Seier, M.; Zimmermann, T. Environmental impacts of decommissioning nuclear power plants: Methodical challenges, case study, and implications. *Int. J. Life Cycle Assess.* **2014**, *19*, 1919–1932. [CrossRef]
19. Kang, H.Y.; Park, S.S.; Han, S.H. Acid corrosion resistance and durability of alkali-activated fly ash cement-concrete. *J. Korean Soc. Environ. Eng.* **2008**, *30*, 61–68.
20. Prošek, Z.; Nežerka, V.; Hlůžek, R.; Trejbal, J.; Tesárek, P.; Karra'a, G. Role of lime, fly ash, and slag in cement pastes containing recycled concrete fines. *Constr. Build. Mater.* **2019**, *201*, 702–714. [CrossRef]
21. Gholampour, A.; Zheng, J.; Ozbakkaloglu, T. Development of waste-based concretes containing foundry sand, recycled fine aggregate, ground granulated blast furnace slag and fly ash. *Constr. Build. Mater.* **2021**, *267*, 121004. [CrossRef]
22. Elchalakani, M.; Bassarir, H.; Karrech, A. Green concrete with high-volume fly ash and slag with recycled aggregate and recycled water to build future sustainable cities. *J. Mater. Civ. Eng.* **2017**, *29*, 04016219. [CrossRef]
23. Majhi, R.K.; Nayak, A.N.; Mukharjee, B.B. Development of sustainable concrete using recycled coarse aggregate and ground granulated blast furnace slag. *Constr. Build. Mater.* **2018**, *159*, 417–430. [CrossRef]
24. Huang, X.; Zhuang, R.L.; Muhammad, F.; Yu, L.; Shiau, Y.C.; Li, D.W. Solidification/stabilization of chromite ore processing residue using alkali-activated composite cementitious materials. *Chemosphere* **2017**, *168*, 300–308. [CrossRef]

25. Jeon, J.H.; Lee, J.H.; Lee, W.C.; Lee, S.W.; Kim, S.O. Evaluation of the solidification of radioactive waste using blast furnace slag as a solidifying agent. *Materials* **2023**, *16*, 6462. [CrossRef]
26. Kim, J.H.; Lee, J.K.; Hyung, W.G. Properties of alkali-activated cement mortar by curing method. *J. Korea Concr. Inst.* **2014**, *26*, 117–124. [CrossRef]
27. Bao, J.; Yu, Z.; Wang, L.; Zhang, P.; Wan, X.; Gao, S.; Zhao, T. Application of ferronickel slag as fine aggregate in recycled aggregate concrete and the effects on transport properties. *J. Clean. Prod.* **2021**, *304*, 127149. [CrossRef]
28. Singh, N.; Singh, S.P. Carbonation resistance and microstructural analysis of low and high volume fly ash self-compacting concrete containing recycled concrete aggregates. *Constr. Build. Mater.* **2016**, *127*, 828–842. [CrossRef]
29. Qin, L.; Gao, X.J. Recycling of waste autoclaved aerated concrete powder in Portland cement by accelerated carbonation. *Waste Manag.* **2019**, *90*, 254–264. [CrossRef]
30. Zhao, P.; Chung, W.; Lee, M.C.; Ahn, S.Y. Experimental study on melt decontamination of stainless steel and carbon steel using induction melting. *Metals* **2021**, *11*, 1218. [CrossRef]
31. Seo, E.A.; Lee, H.J.; Kwon, K.H.; Kim, D.G. Characteristics evaluation of solidifying agent for disposal of radioactive wastes using waste concrete powder. *J. Korean Recycl. Constr. Resour. Inst.* **2021**, *9*, 451–459.
32. *ANS 16.1*; Measurement of the Leachability of Solidified Low-Level Radioactive Wastes by a Short-Term Test Procedure. American Nuclear Society: Downers Grove, IL, USA, 2019.
33. Del Viso, J.R.; Carmona, J.R.; Ruiz, G. Shape and size effects on the compressive strength of high-strength concrete. *Cement Concr. Res.* **2008**, *38*, 386–395. [CrossRef]
34. Sim, J.S.; Park, C.W.; Park, S.J.; Kim, Y.J. Characterization of compressive strength and elastic moduls of recycled aggregate concrete with respect to replacement ratios. *KSCE J. Civ. Eng.* **2006**, *26*, 213–218.
35. McHinnis, M.J.; Davis, M.; Rosa, A.D.L.; Weldon, B.D.; Kurama, Y.C. Strength and stiffness of concrete with recycled concrete aggregates. *Constr. Build. Mater.* **2017**, *15*, 258–269. [CrossRef]
36. *ASTM C39/C39M*; Standard Test Method for Compressive Strength of Cylindrical Concrete Specimens. ASTM International: West Conshohocken, PA, USA, 2020.
37. *KS F 2405*; Standard Test Method for Compressive Strength of Concrete. Korean Standards Association: Seoul, Republic of Korea, 2017.
38. Lo, F.C.; Lo, S.L.; Lee, M.G. Effect of partially replacing ordinary Portland cement with municipal solid waste incinerator ashes and rice husk ashes on pervious concrete quality. *Environ. Sci. Pollut. Res.* **2020**, *27*, 23742–23760. [CrossRef] [PubMed]
39. Hilal, N.; Hadzima-Nyarko, M. Improvement of eco-efficient self-compacting concrete manufacture by recycling high quantity of waste materials. *Environ. Sci. Pollut. Res.* **2021**, *28*, 53282–53297. [CrossRef] [PubMed]
40. Kwon, E.E.; Lee, T.W.; Ok, Y.S.; Tsang, D.C.W.; Park, C.H.; Lee, J.C. Effects of calcium carbonate on pyrolysis of sewage sludge. *Energy* **2018**, *153*, 726–731. [CrossRef]
41. Kim, J.H.; Tae, S.H.; Song, H.; Shin, H.U. Theoretical proposal for the mix design of recycled cement utilizing inorganic construction wastes. *J. Korean Recycl. Constr. Resour. Inst.* **2016**, *4*, 250–258.
42. Park, S.G.; Kwon, S.J.; Kim, Y.M.; Lee, S.S. Reaction properties of non-cement mortar using ground granulated blast furnace slag. *J. Korea Contents Assoc.* **2013**, *13*, 392–399. [CrossRef]
43. Li, B.; Tang, Z.; Huo, B.; Liu, Z.; Cheng, Y.; Ding, B.; Zhang, P. The early age hydration products and mechanical properties of cement paste containing GBFS under steam curing condition. *Buildings* **2022**, *12*, 1746. [CrossRef]
44. Baur, I.; Keller, P.; Mavrocordatos, D.; Wehrli, B.; Johnson, C.A. Dissolution-precipitation behavior of ettringite, monosulfate, and calcium silicate hydrate. *Cement Concr. Res.* **2004**, *34*, 341–348. [CrossRef]
45. Lee, B.K.; Kim, G.Y.; Nam, B.S.; Cho, B.S.; Hama, U.K.; Kim, R.H. Compressive strength, resistance to chloride-ion penetration and freezing/thawing of slag-replaced concrete and cementless slag concrete containing desulfurization slag activator. *Constr. Build. Mater.* **2016**, *128*, 341–348. [CrossRef]
46. Na, H.W.; Moon, K.J.; Hyung, W.G. Application of precast concrete products of non-sintered cement mortar based on industrial by-products. *J. Korea Inst. Build. Constr.* **2020**, *20*, 19–26.
47. Tam, V.W.Y.; Gao, X.F.; Tam, C.M.; Ng, K.M. Physio-chemical reactions in recycle aggregate concrete. *J. Hazard. Mater.* **2009**, *16*, 823–828. [CrossRef]
48. Chen, X.; Wang, G.; Dong, Q.; Zhao, X.; Wang, Y. Microscopic characterizations of pervious concrete using recycled steel slag aggregate. *J. Clean. Prod.* **2020**, *254*, 120149. [CrossRef]
49. Wang, M.; Fu, M.; Li, J.; Niu, Y.; Zhang, Q.; Sun, Q. New insight into polystyrene ion exchange resin for efficient cesium sequestration: The synergistic role of confined zirconium phosphate nanocrystalline. *Chin. Chem. Lett.* **2024**, *35*, 108442. [CrossRef]
50. Zhuang, S.; Mei, Y.; Wang, J. Adsorption performance and mechanisms of Co^{2+} onto carboxyl-functionalized carbon nanotubes. *J. Clean. Prod.* **2023**, *430*, 139709. [CrossRef]
51. Oh, M.; Lee, K.; Foster, R.I.; Lee, C.-H. Feasibility study on the volume reduction of radioactive concrete wstes using thermomechanical and chemical sequential process. *J. Environ. Chem. Eng.* **2021**, *9*, 105742. [CrossRef]

Disclaimer/Publisher's Note: The statements, opinions and data contained in all publications are solely those of the individual author(s) and contributor(s) and not of MDPI and/or the editor(s). MDPI and/or the editor(s) disclaim responsibility for any injury to people or property resulting from any ideas, methods, instructions or products referred to in the content.